iScience, Volume *24*

Supplemental information

Heterocellular spheroids of the neurovascular blood-brain barrier as a platform for personalized nanoneuromedicine

Murali Kumarasamy and Alejandro Sosnik

Supplementary Figures and Tables

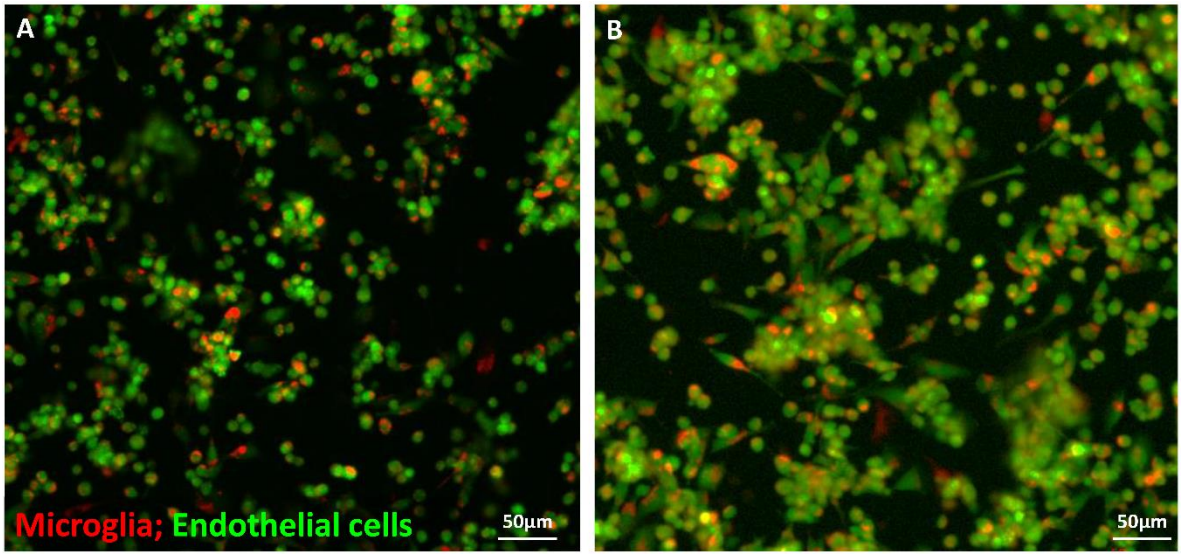

Figure S1. Interspecies interaction of human and rat cells. Related to Figure 1.
CLSFM micrographs of hCMEC/D3 endothelial cells (green) and primary rat microglia (red) stained with Cell Tracking Dye Kit - Green - Cytopainter and Cell Tracking Dye Kit - Deep Red – Cytopainter, respectively, after (A) 1 h and (B) 12 h.

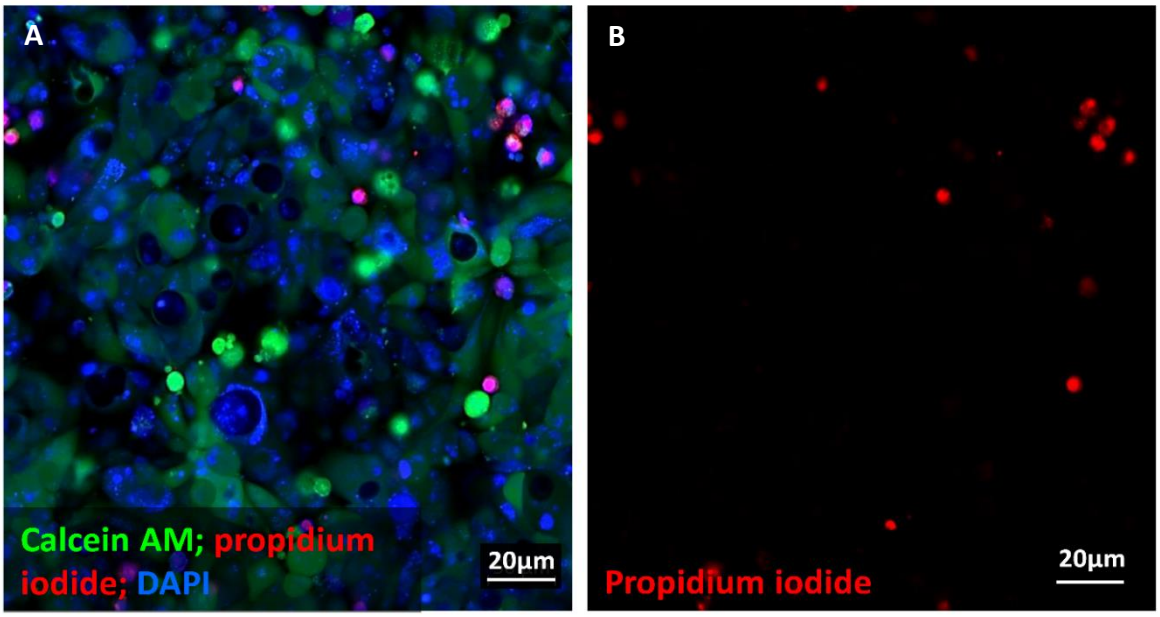

Figure S2. Five-cell spheroid viability. Related to Figure 2.
CLSFM micrographs of 5-cell spheroids stained with (A) calcein AM (live cells, green) and propidium iodide (dead cells, red) and (B) propidium iodide (dead cells, red). Cell nuclei in B-F are stained with 4′,6-diamidino-2-phenylindole (DAPI, blue).

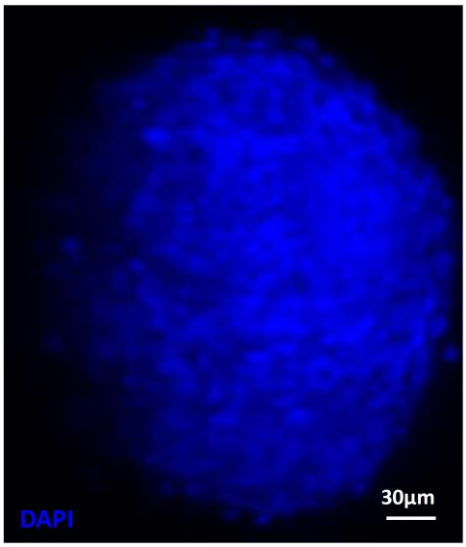

Figure S3. Characterization of the solid cell structure of 5-cell spheroids. Related to Figure 3.
LSFM micrograph of a spheroid showing nuclei of all the cells stained with DAPI (blue).

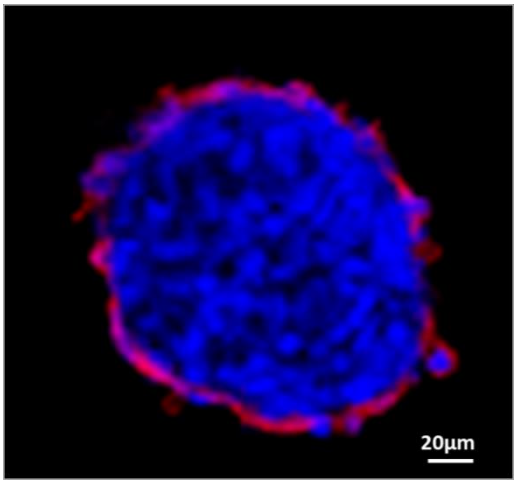

Figure S4. Characterization of hCMEC/D3 endothelial cell distribution in 5-cell spheroids. Related to Figure 3.
CLSFM micrograph of a spheroid showing endothelial cells immunostained for VE-cadherin (red) and nuclei of all the cells stained with DAPI (blue).

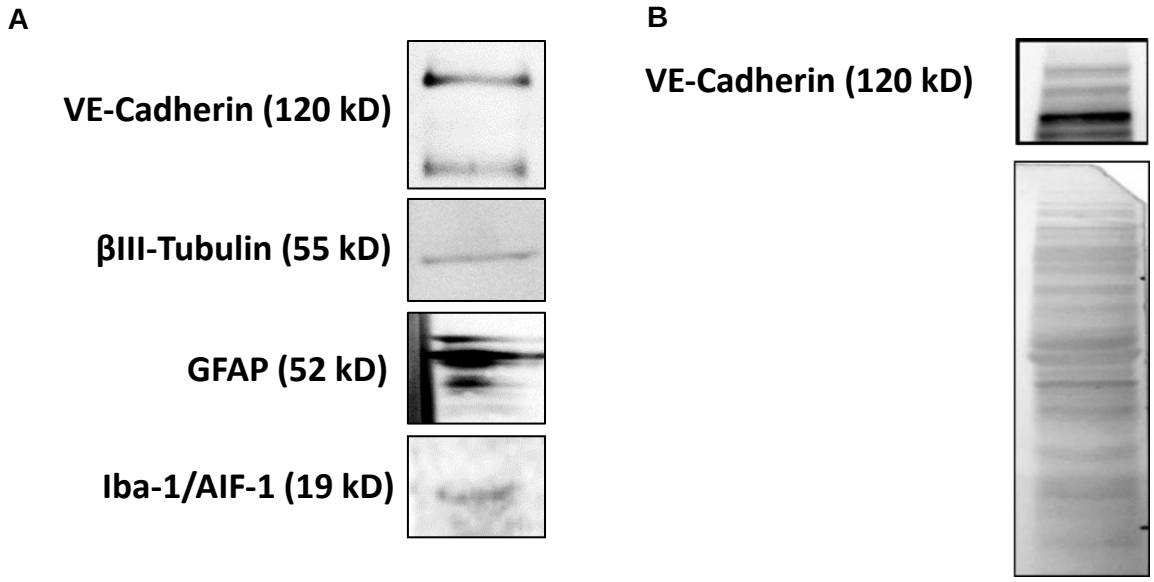

Figure S5. Western blotting analysis of brain specific neurovascular spheroids. Related to Figure 3.
Confirmation of the expression of characteristic protein markers.

Table S1. Quality control of a high-quality total RNA sample by using 1% agarose gel electrophoresis. Related to Figure 6.

Sample number	Sample name	Concentration, (ng/μL) [a]	RIN (TS)
1	Endothelial cells 2D	264	8.5
2	Endothelial cells 2D	116	10
3	Endothelial cells 2D	266	8.5
4	Endothelial cells 3D	110	9.6
5	Endothelial cells 3D	106	9.7
6	Endothelial cells 3D	111	9.6
7	Human 3-cell organoid	69.4	10
8	Human 3-cell organoid	99.4	10
9	Human 3-cell organoid	62.6	10

[a] Determined by Qubit®.
Note: RNA with excellent quality, RIN = 10; RNA with acceptable quality, RIN = 6.9; RNA with poor quality, RIN = 1.8.

Table S2. Technical information and quality of sequencing. Related to Figure 6.

			Quality of Run				
Lane	**Sample**	**Index**	**Control - Mapped (%)**	**Control - Mismatch (%)**	**PF reads (%)**	**Unknown reads (%)**	**Number PF reads**
8	BBB organoids	AGTCAA					25,990,463
		AGTTCC					24,495,706
		GTGGCC					21,842,753
	ECs 2D flat culture	ATGTCA					25,571,133
		CCGTCC	1.46	0.06	91.95	2.18	27,419,486
		GTTTCG					26,094,770
	EC 3D organoids	GTCCGC					25,944,636
		GTGAAA					25,979,188
		CGTACG					22,945,300

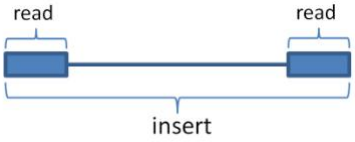

- **Insert** – the DNA/cDNA sequence located between sequencing adapters.

  Read – one end of the paired-end segments.

- **Control -** PhiX is a bacteriophage with a known genome sequence that is used as a standard sequencing control to estimate read accuracy. 1-2% of the reads of each lane are comprised of a PhiX sample which is mapped to the PhiX genome to estimate the error rate and quality of the sequencing run. A good control would have approximately 1% mapped control reads, and up to 1% mismatches (error rate).

- **Unknown reads -** an adapter containing a sample specific barcode is added to each library during library preparation. In some cases, if a read's sequenced barcode contains sequencing errors, then the read cannot be specifically identified with any sample and it is considered as "unknown". The percentage reported in the table is out of the total number of reads per lane.

- **PF** (Passed Filter) **-** indicates reads that passed the automatic quality filter of the sequencer.

Table S3. Trimming statistics. Related to Figure 6.

Sample	Total reads	Containing adapter (%) Reads	Trimmed bases (%)	Reads removed (%)	Reads removed (#)
3-cell BBB organoids	25,990,463	2.6	0.3	0.1	18,349
	24,495,706	2.6	0.3	0.1	17,334
	21,842,753	2.6	0.3	0.1	17,212
ECs 2D-culture	25,571,133	2.6	0.3	0.1	17,660
	27,419,486	2.7	0.3	0.1	19,354
	26,094,770	2.7	0.3	0.1	17,324
EC 3D-organoids	25,944,636	2.7	0.3	0.1	24,616
	25,979,188	2.6	0.3	0.1	21,511
	22,945,300	2.6	0.3	0.1	16,927

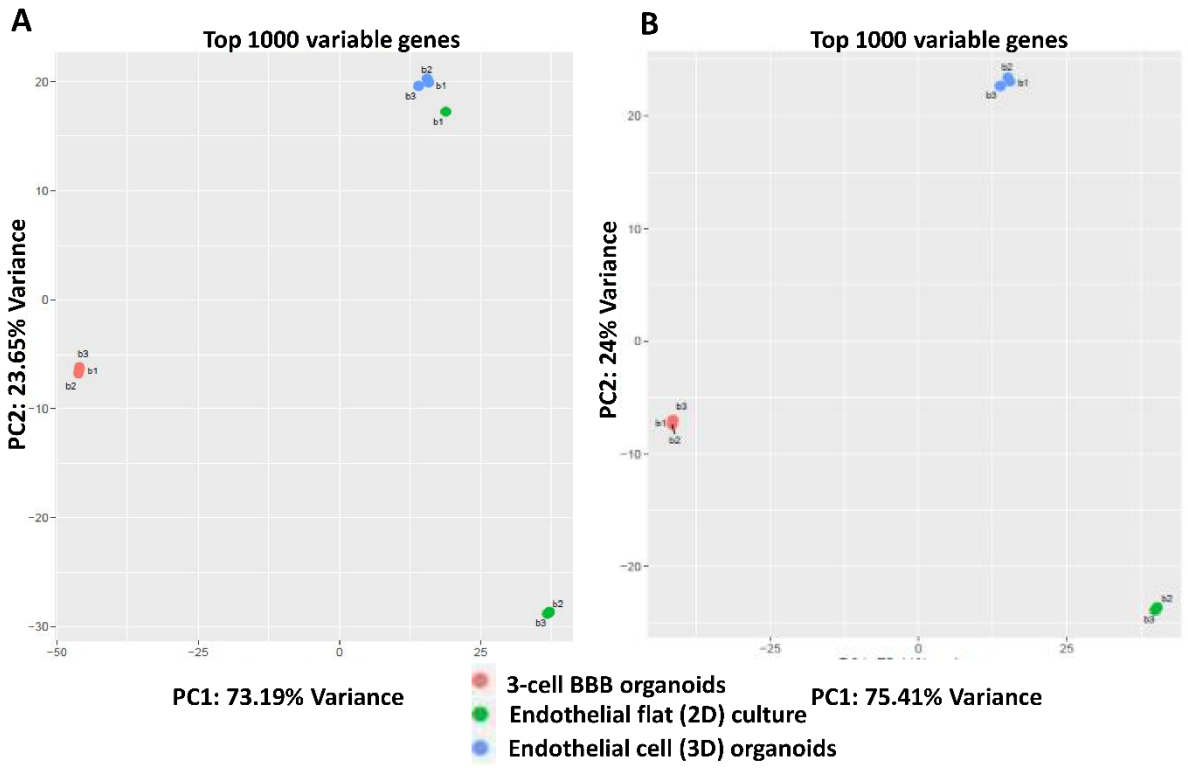

Figure S6. Identification of genes that are most informative for defining cell subpopulations by PCA. Related to Figure 6.
(A) PCA plot between the three groups and (B) PCA plot between groups, after excluding the outlier sample of endothelial flat (2D) culture.

Table S4. Mapping statistics. Related to Figure 6.

Sample	**Total no reads**	% unmapped	% Uniquely unmapped	# Uniquely unmapped	% Multi Mapped	% Gapped Uniquely mapped reads (out of unique)
BBB organoids	25,972,114	1.99	95.12	24,703,511	2.9	20.32
	24,478,372	2.05	95.12	23,283,509	2.83	19.99
	21,825,541	2	95.2	20,777,273	2.8	20.2
ECs 2D flat culture	25,553,473	1.89	95.28	24,347,151	2.84	20.65
	27,400,132	2.56	94.09	25,780,893	3.35	16.81
	26,077,446	2.64	93.87	24,479,978	3.48	16.64
EC 3D organoids	25,920,020	2.15	94.1	24,390,672	3.75	18.86
	25,957,677	2.09	94.65	24,570,220	3.26	19.04
	22,928,373	2.12	94.5	21,668,202	3.38	18.68

•**Uniquely mapped** – Reads aligned with high confidence to a single genomic location with up to 2 mismatches. Only the uniquely mapped reads are used for further analysis.

•**Unmapped** – Reads for which no alignment was found to the reference genome.

•**Multi-mapped** – Reads mapped to more than one possible location in the genome. These reads are not used in the analysis.

•**Gapped uniquely mapping** – Reads aligned uniquely to a splice junction **(Figure. 3)**

Table S5. Differential expression analysis of endothelial cells in 3-human cell spheroids, endothelial cell (3D) spheroids and endothelial cell flat (2D) cultures. Related to Figure 6.
Pairwise testing between conditions.

Comparison	**Total # Genes**	**All Zero**	**Low Counts**	**Tested**	**Significant up-regulation**	**Significant down-regulation**
3-Human cell spheroids vs._ endothelial cell flat (2D) cultures	58,174	22,654	15,211	20,309	7314	6273
3-Human cell spheroids vs._ endothelial cell (3D) spheroids	58,174	22,654	16,294	19,226	3966	3487
Endothelial cell flat (2D) cultures vs._ endothelial cell (3D) spheroids	58,174	22,654	15,849	19,671	6290	6503

Table S6. Comparative expression of different characteristic genes of endothelial cells in 3-human cell spheroids, endothelial cell (3D) spheroids and endothelial cell flat (2D) cultures, as determined by RNA-Seq. Related to Figure 6.

Gene	3-Human cell spheroids vs. endothelial cell flat (2D) cultures	3-Human cell spheroids vs. endothelial cell (3D) spheroids	Endothelial cell flat (2D) cultures vs. endothelial cell (3D) spheroids
GJA1	Upregulated	Upregulated	Downregulated
EDN1	Upregulated	Upregulated	Downregulated
VWF	Upregulated	Downregulated	Downregulated
CD34	Upregulated	Downregulated	Downregulated
ENG	Upregulated	Upregulated	Downregulated
VCAM1	Upregulated	No change	Downregulated
EMCN	Upregulated	Upregulated	No change
NR2F2	Upregulated	Upregulated	Downregulated
CDH5	Upregulated	Downregulated	Downregulated
GJA4	No change	No change	No change
EPHB4	Upregulated	Downregulated	Downregulated
MCAM	Upregulated	Upregulated	Downregulated
FLT1	No change	Downregulated	No change
NOS3	No change	No change	No change
FLT4	No change	No change	No change
PTPRC	No change	No change	No change
CD4	Upregulated	Upregulated	No change
ICAM3	No change	No change	No change
BCL6	Upregulated	Upregulated	Upregulated
CD28	No change	No change	No change
ITGA4	Up	Upregulated	Downregulated
CD38	No	Upregulated	No change
CD86	No	No change	No change
MS4A1	No	No change	No change

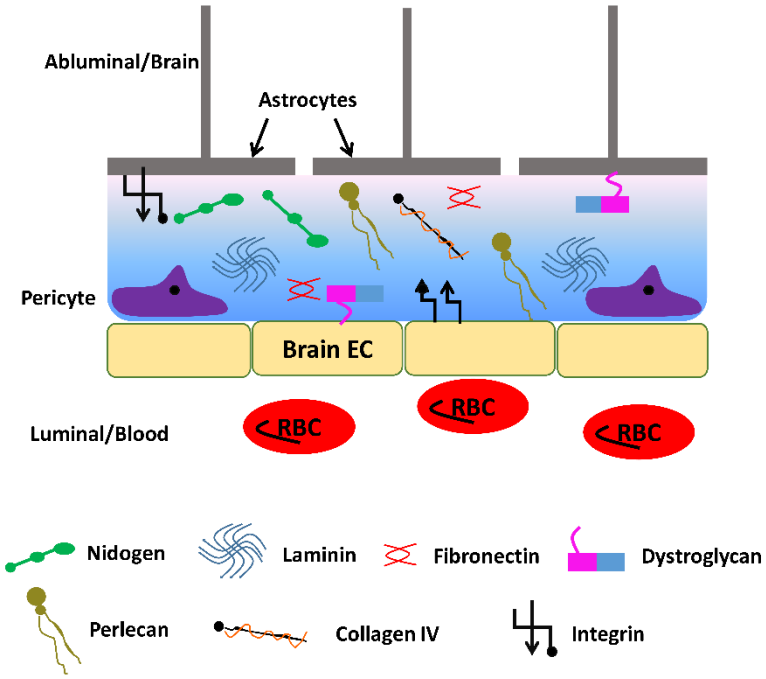

Figure S7. Scheme of the extracellular matrix (ECM) in the vascular and parenchymal basement membrane of endothelial cells (EC) and red blood cells (RBC). Related to Figure 6.
Key proteins are indicated.

Table S7. Properties of the different polymeric, metallic and carbon nanoparticles used to investigate the interaction of nanomaterials with 5-cell spheroids. Related to Figures 7 and 8.

Nanoparticle type	D_h (nm) ± S.D.	PDI	Z-potential (mV)	Nanoparticle description
Polymeric				
CS-PMMA33	188 ± 9	0.30	+23.0	Non-crosslinked amphiphilic nanoparticles produced by the self-assembly of a graft copolymer of chitosan (CS) and poly(methyl methacrylate) (PMMA) containing 33% w/v of PMMA (Noi et al., 2018)
Crosslinked mixed CS-PMMA30:PVA-PMMA17	463 ± 73	0.55	+3.0	Mixed amphiphilic nanoparticles produced by the self-assembly of a 1:1 weight ratio mixture of a graft copolymer of chitosan (CS) and poly(methyl methacrylate) (PMMA) containing 30% w/v of PMMA and a graft copolymer of poly(vinyl alcohol) (PVA) and PMMA containing 17% w/v of PMMA. Nanoparticles were ionotropically crosslinked with sodium

				tripolyphosphate which reacts with CS domains (Schlachet and Sosnik, 2019)
Crosslinked PVA-PMMA17	92 ± 4	0.14	-14.6	Amphiphilic nanoparticles produced by the self-assembly of a graft copolymer of poly(vinyl alcohol) (PVA) and poly(methyl methacrylate) (PMMA) containing 17% w/v of PMMA (Moshe Halamish et al., 2019). Nanoparticles were non-covalently crosslinked with boric acid which reacts with PVA domains (Moshe Halamish et al., 2019)
hGM-PMMA28	141 ± 3	0.11	-0.4	Amphiphilic nanoparticles produced by the self-assembly of a graft copolymer of hydrolyzed galactomannan (hGM) and poly(methyl methacrylate) (PMMA) containing 28% w/v of PMMA (Zaritski et al., 2019)
Metallic				
Silver	60 ± 13		-38.0	An aqueous solution of silver nitrate was heated to boiling, sodium citrate and sodium borohydride was

				added slowly (Bastús et al., 2014; Quintero-Quiroz et al., 2019)
Gold	10 ± 2	<0.20	-17.8	Commercially available
Ceramic				
Graphene nanoplatelets	~5 µm diameter and 10 nm thickness	-	-	Commercially available
Alkaline carbon dots	10 ± 3	0.20	−12.0 mV	Sodium hydroxide was mixed with acetone under vigorous magnetic stirring for 1 h, and then the mixture was placed at ambient air, temperature, and pressure. The product was separated by centrifugation and washed to get a powder of alkaline quantum dots (Hou et al., 2015).

Figure S8. Per-base quality scores. Related to Figure 6.

Table S8. Read assignments according to gene annotations. Related to Figure 6.

Sample	**# reads unique**	% reads unique	# no feature	% no feature	Number ambiguous	%ambiguous
BBB organoids	21,478,458	86.94	1,734,480	7.02	1,490,573	6.03
	20,218,632	86.84	1,679,234	7.21	1,385,643	5.95
	18,066,504	86.95	1,453,586	7	1,257,183	6.05
ECs 2D flat culture	21,637,878	88.87	1,182,240	4.86	1,527,033	6.27
	21,594,711	83.76	2,686,051	10.42	1,500,131	5.82
	20,471,953	83.63	2,580,918	10.54	1,427,107	5.83
EC 3D organoids	20,884,278	85.62	2,006,406	8.23	1,499,988	6.15
	21,168,497	86.16	1,863,925	7.59	1,537,798	6.26
	18,520,642	85.47	1,809,475	8.35	1,338,085	6.18

•**Counted reads** – uniquely mapped reads assigned to annotated exons.

•**No feature** – reads that could not be assigned to any annotated gene.

•**Ambiguous –** reads that can be assigned to more than one annotated gene and are therefore not counted to any gene.

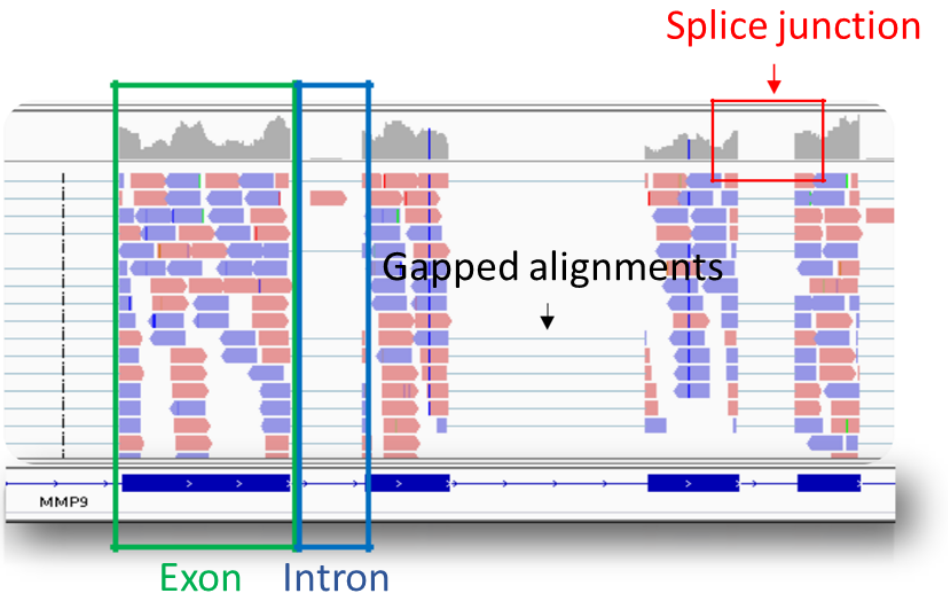

Figure S9. Illustration of RNA-Seq read alignments using Tophat2 – A graphic representation of the mapping patterns of RNA-Seq reads to a reference genome. Related to Figure 6.
The figure above reveals the distribution of reads that are mapped to exons (outlined in green), a splice junction (outlined in red), and introns (outlined in blue). The figure allows the user to see that the majority of reads map to exons, slightly fewer reads map in a gapped manner to the pictured splice junction, and—consistent with the nature of RNA library preparation preference for mature mRNAs—almost no reads map to introns.

Transparent Methods

Cell cultures

The hCMEC/D3 cell line derived from human temporal lobe microvessels (hBMECs, EMD Millipore, Burlington, MA, USA) was maintained in EndoGRO Basal Medium (EMD Millipore) with supplements containing 5% fetal bovine serum (FBS), L-glutamine, vitamin C, heparin sulfate and recombinant human epidermal growth factor (*rhEGF*), all purchased from Sigma-Aldrich (St. Louis, MO, USA). hAs (ScienCell Research Laboratories, Carlsbad, CA, USA) were grown in astrocyte growth medium (ScienCell Research Laboratories) containing 2% FBS supplemented with astrocyte growth factors, penicillin-streptomycin (Brissette et al., 2013) hBVPs (ScienCell Research Laboratories) were maintained in pericyte culture medium (ScienCell Research Laboratories) containing 2% FBS, pericyte growth supplement and penicillin-streptomycin (Neuhaus et al., 2017). All cells were incubated at 37°C in humidified 5% CO_2/95% air.

Animals and isolation of primary neural-tissue cells

The use of neonate Sprague-Dawley (SD) rats (P0-1) and the protocols utilized for the isolation of the primary CNS cells were conducted with the approval of the Animal Care Committee of the Technion-Israel Institute of Technology. All the experimental procedures were in accordance with the guidelines set by the EU Council Directive (86/609 EEC) and according to the official protocol #IL-141-10-17 (expiry date 19 December 2021).

Primary neural, and neural stem/progenitor cells (Beaudoin et al., 2012; Seibenhener and Wooten, 2012) were isolated from P0-1 SD rats. Briefly, rats were sacrificed by decapitation, and whole brains were quickly removed aseptically (SZ09010122 Binocular Zoom Stereo Microscope, 8x~50x, YSC Technologies, Fremont, CA, USA). Cerebral cortices of three pups were dissected under sterile conditions and kept on ice in a sterile Falcon tube (15 mL) containing 3 mL of trypsin-EDTA 0.25% (Sigma-Aldrich) for 10 min. The enzyme solution was aspirated, and enzyme-digested tissues were triturated in 10 mL of warm (37°C) Dulbecco's Modified Eagle Medium *(*DMEM, Sigma-Aldrich) containing 10% heat-inactivated FBS. Cortical neuron cultures were dissociated by trituration using a 10 mL pipette (about 15-20 times) and cells were centrifuged (Z300 Hermle Micro Centrifuge, Hermle AG, Gosheim, Germany) at 4°C (1500g, 5 min) to obtain pellets. Single cells were separated from non-dissociated tissue debris by sieving them through Falcon™ Cell Strainers (pore diameter of 70μm, Sigma-Aldrich) and seeded onto 24- or 96-well plates coated with poly-L-lysine-

(PLL, Sigma-Aldrich) at cell densities of 2×10^5 or 1×10^4 cells/well, respectively. Cultures were incubated at 37°C in a humidified atmosphere of 5% CO_2/95% air. Cultured cells were grown in serum-free neuron-specific DMEM and Ham's F12 nutrient mixture (DMEM: F12 1:1, Sigma-Aldrich) supplemented with 1% v/v insulin-transferrin-selenite (ITS, Sigma-Aldrich). For conventional cultures and bioimaging, the dissociated cultures were plated on glass coverslips in 24-well plates (Paul Marienfeld GmbH & Co. KG., Lauda-Königshofen, Germany). Before culture, glass coverslips were washed in water and 96% ethanol, air-dried, placed in 24-well plates, and coated with PLL overnight. The cell composition of the cultures was characterized by immunocytochemical staining for neuron specific biomarkers. Microglial cultures were prepared according to Saura *et al.* (Saura et al., 2003). Briefly, P0-1 SD rat brains were removed and rinsed in phosphate buffer saline (PBS, Sigma-Aldrich). After careful removal of the meninges and brains cortices, they were mechanically dissociated and trypsinized for 20 min. Cells were cultured in 6-well plates with DMEM containing 10% FBS at 37°C in humidified 5% CO_2/95% air. The medium was exchanged twice weekly. Microglia cells were isolated from mixed glia by mild trypsinization (30 min-2 h) with trypsin-EDTA 0.25% diluted 1:3 in serum-free DMEM, at 37°C. After detachment of astrocyte brown sheets, the firmly attached macrophages were further propagated in DMEM:F12 1:1 with 10% FBS and the cells replated in 24-well plates containing PLL-coated glass coverslips at a density of 50,000 cells/well. For microglia stainings, cells were fixed and the immunostaining and imaging were performed according to the protocol described below.

Assembly of heterocellular spheroids

Three-cell spheroids comprising hCMEC/D3, hAs and hBVPs were cultured in EndoGRO Basal Medium supplemented with 5% FBS, L-glutamine, vitamin C, heparin sulfate and rhEGF, at 37°C in humidified 5% CO_2/95% air using the liquid overlay culture system. We used the same method to produce 5-cell spheroids incorporating primary neurons and microglia isolated from neonate rat (see above). This method is our adaptation of the aggregate cultures previously described (Johnstone et al., 1998). Briefly, the three or five cell types were harvested by trypsin-EDTA 0.25% and resuspended in ENDOGro culture medium. The concentration of hECs, hAs, hBVPs, primary neurons and microglia cells in each individual suspension was determined using a haemocytometer. Then, cells were resuspended in 100 µL of medium at a 4:2:1:1:1 ratio and transferred to ultralow attachment (ULA) round bottom 96-well plates (CellCarrier Spheroid ULA 96-well Microplates, PerkinElmer, Waltham, MA, USA). In another method, we prepared a 1% w/v agarose solution (molecular biology grade, Bio-Rad

Laboratories, Hercules, CA, USA) in PBS under boiling until complete dissolution. The agarose solution (100 μL) was pipetted into each well of a 96-well plate, while it was still hot, and allowed to cool to 37°C and solidify. Then, a suspension of 5-cell spheroids contains hCMEC/D3, hAs, hBVPs, and primary neurons and microglia cells at a 4:2:1:1:1 ratio and hCMEC/D3 endothelial cells, hAs and hBVPs (1:1:1 ratio), was seeded in the 96-well plate. In both methods, cells were incubated in ENDOGro medium, at 37°C in humidified 5% CO_2/95% air for 48–72 h to allow the formation of the spheroids, as exemplified for a 5-cell spheroid produced in round bottom 96-well plate in **Video S1**.

To rule out possible detrimental human-rodent cell interactions during spheroid assembly, hCMEC/D3 and primary rodent microglia cells were labeled with Cell Tracking Dye Kit - Green - Cytopainter (ab138891, Abcam, Cambridge, UK) and Cell Tracking Dye Kit - Deep Red - Cytopainter (ab138894, Abcam), respectively, and imaged by a GE InCell Analyzer 2000 Imaging System (GE Healthcare, Chicago, IL, USA). For the staining, cells were mixed with each dye (1:1000 dilution in PBS) for 10 min, at 37°C in humidified 5% CO_2/95% air, washed thrice with ENDOGro culture medium and co-cultured on CellCarrier Spheroid ULA 96-well Microplates to form 2-cell spheroids. Images were acquired with a 10x objective at the end of each illumination period (every 10 min) for 12 h.

Characterization of heterocellular spheroids

LIVE/DEA assay

Heterocellular spheroids were resuspended at day 3, the cell viability was determined by using a calcein-AM/propidium iodide LIVE/DEAD assay and nuclei stained with DAPI (all supplied by Sigma-Aldrich). Briefly, the cell culture medium was removed and 1 μM calcein AM and 1.5 μM propidium iodide were added in each well, and the spheroids gently resuspended and incubated for 20 min, at 37°C. Spheroids were visualized by CLSFM (LSM 710 microscope, Carl Zeiss AG, Oberkochen, Germany). Fluorescence mean intensities of both live and dead cells were estimated by ImageJ software (National Institutes of Health, MD, USA).

Immunofluorescent labeling

Spheroids and monocultures were collected at day 5, pooled into a 0.2 mL Eppendorf tube (Corning Inc., Corning, NY, USA), washed thrice (5 min) with PBS and fixed in 4% w/v paraformaldehyde (PFA, Sigma-Aldrich) for 15 min at room temperature (RT). Fixed spheroids were washed twice in PBS, permeabilized with 0.1% w/v Triton X-100 (Sigma-

Aldrich) solution in PBS and blocked with 1% w/v bovine serum albumin (BSA, Sigma-Aldrich) for 1 h. Then, spheroids were incubated in mixtures of primary antibodies overnight at RT under constant rotation, washed thrice with PBS, incubated overnight at 4°C in a mixture of secondary antibodies, all diluted in blocking solutions. Finally, the remainders of secondary antibodies were washed with PBS before staining cell nuclei with DAPI.

Immunolabeled spheroids were visualized by using a LSM 710 microscope equipped with 10x, 20x, 40× water 1.4 NA and 63× oil (numerical aperture:1.3) Carl Zeiss objectives (as indicated in the corresponding figure legends). We used 405, 488, 561 and 647 nm lasers, and the scanning was done in line serial mode, pixel size was 50 x 50 nm. Image stacks were obtained with Zen Elements software. Whole-spheroid images were acquired using a 10× magnification objective and images were processed by using the Zen 100 software.

The following commercial primary antibodies were used at a concentration of 1:500: (i) βIII-tubulin (AA10, sc-80016; Santa Cruz Biotechnology, Inc., Dallas, TX, USA), (ii) GFAP (sc-33673, Santa Cruz), (iii) AQP4 (sc-390488 Santa Cruz), (iv) CLDN5 (sc-374221, Santa Cruz), (v) Iba-1/AIF-1 (sc-32725, Santa Cruz), (vi) VE-cadherin (ab33168, Abcam), (vii) iNOS (ab15323; Abcam), (viii) MAP-2 (sc-74421, Santa Cruz), and (ix) NG2 (sc-53389, Santa Cruz). The following commercial secondary antibodies were used at a concentration of 1:1000: (i) goat anti-rabbit IgG H&L (Alexa Fluor® 594, ab150080, Abcam), (ii) mouse IgG kappa binding protein (m-IgGκ BP) conjugated to CruzFluor™ 488 (sc-516176, Santa Cruz), (iii) mouse IgG kappa binding protein (m-IgGκ BP) conjugated to CruzFluor™ 555 (sc-516177, Santa Cruz), and (iv) mouse IgG kappa binding protein (m-IgGκ BP) conjugated to CruzFluor™ 647.

This method was also used to characterize the permeability of selected polymeric NPs and their localization within the spheroid. For this, NPs were synthesized by utilizing copolymers fluorescently-labeled by the conjugation of fluorescein isothiocyanate (FITC, green fluorescence, Sigma-Aldrich) or rhodamine isothiocyanate (RITC, red fluorescence Sigma-Aldrich) (Moshe Halamish et al., 2019; Noi et al., 2018; Schlachet and Sosnik, 2019; Zaritski et al., 2019).

Electron microscopy

Spheroids were established for 24-72 h and collected and pooled in an Eppendorf tube. Then, they were washed once with PBS, and immersed in modified Karnovsky's fixative (2% w/v glutaraldehyde and 3% w/v PFA in 0.1 M sodium cacodylate buffer containing 5mM $CaCl_2$

and 3% sucrose, all from Sigma-Aldrich) for 1 h at RT. Spheroids were washed in 0.1 M cacodylate buffer and fixed with 1% w/v osmium tetroxide (Sigma-Aldrich)/0.5% w/v potassium dichromate (1 h), stained with 1% w/v uranyl acetate (1 h), washed twice with water and dehydrated in ethanol (Bio-Lab Ltd., Jerusalem, Israel) according to the following sequence: 50% (10 min), 70% (10 min), 90% (10 min) and 100% (2 × 10 min). Samples were embedded in EMbed 812 resin (Electron Microscopy Sciences, Hatfield, PA, USA) and polymerized at 60°C for 48 h (Douglas and Elser, 1972; Murray et al., 1991; Phillips, 1998). Ultrathin sections (~70 nm) were produced in an ultra-microtome (Leica Biosystems, Buffalo Grove, IL, USA), transferred to copper grids (Sigma-Aldrich) and visualized by using a Zeiss Ultra-Plus FEG-SEM (Carl Zeiss AG) equipped with STEM detector at accelerating voltage of 30 kV. This method was also used to characterize the permeability and the intracellular fate of model metallic and ceramic NPs in the spheroids and enabled the elucidation of ultrastructural details and mechanisms of NP–spheroid interactions.

Light sheet fluorescence microscopy

Spheroids fixed in 4% w/v PFA and immunostained were embedded in 1% w/v low melting agarose (Bio-Rad Laboratories) solution and placed in an Eppendorf tube. Samples were analyzed by using a ZEISS Lightsheet Z.1 Fluorescence Microscope (Carl Zeiss) with the Sampler Starter Kit containing four color coded sleeves with their corresponding plungers to fit the glass capillaries high optical clarity for the 3D imaging to the sample holder. Upon selection of the proper capillary based on the sample size and plunger assembly, a 1% w/v low melting agarose solution (100 μL) in sterile PBS was mixed with the spheroid, plunged into the capillary and allowed to polymerize at RT. Finally, the sample was pushed out and mounted in the sample chamber of the microscope at 37°C in 5% CO_2/95% air for imaging. This method was also used to characterize the interaction of FITC- or RITC-labeled polymeric nanoparticles with the spheroids. LSFM images were deconvolved using IMARIS Professional software (https://imaris.oxinst.com/).

Time-lapse video microscopy

We used video microscopy to evaluate the interspecies interaction between hCMEC/D3 and rat microglia cells. For this, these two cells were co-cultured on low-attachment agarose coated 96-well plates or CellCarrier Spheroid ULA 96-well plates with special optical bottom to form spheroids (see above). Cultures were kept at 37°C in humidified 5% CO_2/95% air within a mini-incubator attached to the microscope stage. Time-lapse videos were recorded in both phase-contrast optical, and fluorescence modes using Alexa® Fluor 488 and 594 and DAPI

nuclear staining by using the InCell Analyzer 2000. Twenty-thirty individual cells were chosen in every starting microscopic image for cell-cell interactions. Images were acquired with a 10x objective at the end of each illumination period (every 10 min) for 24 h. Obtained digital images and image sequences were translated into a video format (AVI).

Total RNA sequencing and data processing

At the end of day 5, total RNA was extracted from BBB spheroids using a T-series Ultraclear 1.5 mL Microcentrifuge tube (Scientific Specialties, Inc., Lodi, CA, USA). The spheroid pellet was immersed in 500 µL of TRIzol (Invitrogen, Carlsbad, CA, USA) following the manufacturer's instructions and stored at -80°C until further use. Samples were analysed in triplicates for RNA-Seq analysis. RNA-Seq libraries were constructed by using Illumina HiSeq 2500 Stranded Total RNA TruSeq RNA Library Preparation Kit v2 (Illumina, San Diego, CA, USA) and sequenced on the Illumina Nova Seq 6000 platform in the SR 50bp and barcode (Illumina). Total RNA-seq was performed from three replicates of 1-cell (only endothelial) and 5-cell spheroids.

For gene expression analyses, trimmed reads with cutadapt were aligned to the reference genome (hg38UCSCassembly) using FASTQC version 0.11.5 (uses cutadapt version 1.10, Brabraham Bioinformatics, Cambridge, UK) and Tophat2 version 2.1.0 (uses Bowtie2 version 2.2.6, Johns Hopkins University, Baltimore, MD, USA), with default parameters and Ref Seq annotation (genome-build GRCh38.p9). The distribution of alignments was analysed using Cufflinks version 2.2.1 (Trapnell Lab, University of Washington, Seattle, WA, USA) and fragments per kilo base of exon model per million reads mapped values were quantile normalized. The quality control of the sequenced data (quality of all sequenced bases, trimming and mapping statistics in all reads) was evaluated using FASTQC version 0.11.5 (**Tables S1-S3**). The minimal quality threshold was set to 20 (phred scale) and the selected TruSeq RNA adapter sequence was: AGATCGGAAGAGC. The quality scores are presented as Phred values (10 log10P base call is wrong), i.e., values higher than 30 indicate a probability of less than 10^{-3} of an incorrect base call (**Figure S8**).

Only unique mapped reads were counted to genes, using 'HTSeq-count' package version 0.6.1 with 'union' mode. Normalization and differential expression analyses (**Table S8**) were conducted using DESeq2 R package version 1.18.1. The reads were mapped to the Homo sapiens (human) genome assembly *GRCh38* (hg38) from Genome Reference Consortium (ftp://ftp.ensembl.org/pub/release-96/fasta/homo_sapiens/) using Tophat2 version 2.1.0 (uses

Bowtie2 version 2.2.6), with up to maximum of 3 mismatches allowed per read, the minimum and maximum intron sizes were set to 70 and 50,000, respectively, and an annotation file was provided to the mapper (**Figure S9**). Replicates were analyzed by the similarity between the suggested replicates and explore the relations between the samples, heatmaps and Principal Component Analysis (PCA) plots were generated by a plot that span(s) the samples in 2D plane by their first two principal components (**Figure S6**).

Protein expression analysis

Five-cell spheroids were collected and washed with PBS several times and lysed by adding a NP-40 lysis buffer (Thermo Fisher Scientific) to conduct Western Blot analysis. Cell lysates were centrifuged (16,800g, 4°C) in a table-top centrifuge (Eppendorf, Hamburg, Germany) and stored at −80°C until use. Protein concentrations were determined by Bradford protein assay (Bio-Rad Laboratories) and SDS-PAGE was performed according to standard protocols. In each lane, total protein was loaded, and 10% or 15% SDS-PAGE gels were used. Gels were transferred to nitrocellulose membranes (GE Healthcare Life Sciences, Marlborough, MA, USA), blocked with 5% w/v non-fat milk (Sigma-Aldrich) for 1 h at RT, washed and incubated with the selective potentially associated primary antibody for overnight at 4^0C (see above for antibodies list). Membranes were washed and incubated with the respective secondary HRP conjugate antibody (Bio-Rad Laboratories) for chemiluminescence analysis with an Image Quant LAS 4000 camera (GE Healthcare Life Sciences). The following primary antibodies were used at a concentration of 1:500: (i) βIII-tubulin antibody, (ii) GFAP, (iii) Iba-1/AIF-1 and (iv) VE-cadherin.

The nanoparticles

In this work, we utilized different polymeric, metallic and carbon nanoparticles to assess their permeability in 5-cell spheroids.

Polymeric nanoparticles

Different polymeric NPs were obtained by the self-assembly of amphiphilic graft copolymers of chitosan (CS), poly(vinyl alcohol) (PVA) and hydrolyzed galactomannan (hGM) with poly(methyl methacrylate) (PMMA). The copolymers were synthesized by the free radical graft polymerization of methyl methacrylate (MMA) initiated by cerium(IV) ammonium nitrate (CAN) in acid aqueous medium. For this, CS, PVA or hGM (0.4 g) was dissolved in nitric acid solution in water (0.05 M). Then, tetramethylethylenediamine (0.18 mL) was diluted in distilled water (50 mL) in a closed round-bottom flask protected from light. Then, both

solutions were degassed separately by sonication for 30 min (Elmasonics S 30, Elma, Singen, Germany), mixed, purged with N_2 gas for 30 min at room temperature, and heated to 35 °C, and the corresponding amount of MMA (according to the desired weight feed ratio) was directly poured into the solution. Finally, a CAN solution (0.66 g in 2 mL of degassed water) was added, and the reaction was carried out under a N_2 environment (3-6 h, 35 °C). The polymerization was finalized by the addition of hydroquinone (0.132 g). Reaction crudes were dialyzed against water (regenerated cellulose dialysis membranes; MWCO, 3500 Da) in 100-fold volume of the dialyzed solution and freeze-dried (72−96 h). Products were stored at 4 °C until use (Moshe Halamish et al., 2019; Noi et al., 2018; Schlachet and Sosnik, 2019; Zaritski et al., 2019).

Metallic nanoparticles

Au NPs (diameter of 10 nm, Sigma-Aldrich) and Ag NPs (diameter of 60 nm) synthesized from silver nitrate by reduction with sodium borohydride and stabilization with sodium citrate (all supplied by Sigma-Aldrich) (Bastús et al., 2014; Quintero-Quiroz et al., 2019) were utilized as prototypes of metallic NPs.

Carbonaceous nanoparticles

We used graphene nanoplatelets (diameter of ~5 μm and thickness of ~100 nm, GNN P0205, Ants Ceramics Pvt. Ltd., Vasai-Virar, India) and alkaline carbon dots produced by the reaction of acetone with sodium hydroxide (Hou *et al.*) (Hou et al., 2015) Briefly, NaOH (8 g, Sigma-Aldrich) was mixed with acetone (40 mL, Bio-Lab Ltd., Netanya, Israel) under magnetic stirring (1 h). Then, the mixture was stored at ambient air and RT (5 days) and the pH adjusted to 7 with HCl solution (1 M, Bio-Lab Ltd.) was added to adjust the pH to be neutral. Carbon dots were separated by centrifugation and washed with water several times, and the product dried at 100 °C for 12 h.

The size (hydrodynamic diameter, D_h) and size distribution (polydispersity, PDI) of the different nanoparticles before the biological studies were measured by dynamic light scattering (DLS, Zetasizer Nano-ZS, Malvern Instruments, Malvern, UK) in 10 mm quartz cuvettes using a He-Ne laser (673 nm) as light source at a scattering angle of 173°, at 25°C. Data were analyzed using CONTIN algorithms (Malvern Instruments). The surface charge was estimated by measuring the zeta-potential (Z-potential) by laser Doppler micro-electrophoresis in the Zetasizer Nano-ZS. Each value is expressed as mean ± S.D. of at least three independent samples, while each DLS or Z-potential measurement is an average of at least seven runs. For

biological studies, copolymers were fluorescently-labeled with FITC or RITC, both from Sigma-Aldrich (Moshe Halamish et al., 2019; Noi et al., 2018; Schlachet and Sosnik, 2019; Zaritski et al., 2019). The properties of the NPs used in this work are summarized in **Table S7**. Before use, NPs were diluted under sterile conditions and mixed with the corresponding culture medium to the final desired concentration.

Statistical Analysis

RNA-Seq data to compare between spheroid groups was obtained from three biological replicates. Wald test parameters were used for pairwise comparisons. The statistical analysis was conducted and the log2 fold change and the adjusted p-values (p_{adj}) were indicated for significantly upregulated and downregulated genes; $p_{adj} < 0.05$ was considered statistically significant. The differential expression analysis was conducted using 'DESeq2' R software. The Zen software was used to evaluate CLSFM and LSFM images. In some cases, the TIFF images acquired with IMARIS software were imported for subsequent measurement and analysis. Results are expressed as mean ± S.D. of three experimental replicates performed under the same conditions (n = 3), unless otherwise specified. All cellular measurements and subsequent analyses were performed in a blinded manner and cell counts and image processing for all experimental conditions were carried out in triplicate. CT values and normalized gene expression values were taken after analysis and the data were exported to Excel (Microsoft, Seattle, WA, USA) spreadsheet software for expression units and S.D. analysis.

References

Bastús, N.G., Merkoçi, F., Piella, J., and Puntes, V. (2014). Synthesis of Highly Monodisperse Citrate-Stabilized Silver Nanoparticles of up to 200 nm: Kinetic Control and Catalytic Properties. Chemistry of Materials *26*, 2836-2846.

Beaudoin, G.M., 3rd, Lee, S.H., Singh, D., Yuan, Y., Ng, Y.G., Reichardt, L.F., and Arikkath, J. (2012). Culturing pyramidal neurons from the early postnatal mouse hippocampus and cortex. Nat Protoc *7*, 1741-1754.

Brissette, C.A., Kees, E.D., Burke, M.M., Gaultney, R.A., Floden, A.M., and Watt, J.A. (2013). The multifaceted responses of primary human astrocytes and brain microvascular endothelial cells to the Lyme disease spirochete, Borrelia burgdorferi. ASN Neuro *5*, 221-229.

Douglas, W.H., and Elser, J.E. (1972). A method for in situ embedding of cultured cells grown on plastic surfaces. In Vitro *8*, 26-29.

Moshe Halamish, H., Trousil, J., Rak, D., Knudsen, K.D., Pavlova, E., Nyström, B., Štěpánek, P., and Sosnik, A. (2019). Self-assembly and nanostructure of poly(vinyl alcohol)-graft-poly(methyl methacrylate) amphiphilic nanoparticles. Journal of Colloid and Interface Science *553*, 512-523.

Hou, H., Banks, C.E., Jing, M., Zhang, Y., and Ji, X. (2015). Carbon Quantum Dots and Their Derivative 3D Porous Carbon Frameworks for Sodium-Ion Batteries with Ultralong Cycle Life. Advanced Materials *27*, 7861-7866.

Johnstone, B., Hering, T.M., Caplan, A.I., Goldberg, V.M., and Yoo, J.U. (1998). In vitro chondrogenesis of bone marrow-derived mesenchymal progenitor cells. Exp Cell Res *238*, 265-272.

Murray, A.B., Schulze, H., and Blauw, E. (1991). In situ embedding of cell monolayers cultured on plastic surfaces for electron microscopy. Biotech Histochem *66*, 269-272.

Neuhaus, A.A., Couch, Y., Sutherland, B.A., and Buchan, A.M. (2017). Novel method to study pericyte contractility and responses to ischaemia in vitro using electrical impedance. J Cereb Blood Flow Metab *37*, 2013-2024.

Noi, I., Schlachet, I., Kumarasamy, M., and Sosnik, A. (2018). Permeability of Novel Chitosan-g-Poly(Methyl Methacrylate) Amphiphilic Nanoparticles in a Model of Small Intestine In Vitro. Polymers (Basel) *10*, 478.

Phillips, D.M. (1998). Electron microscopy: use of transmission and scanning electron microscopy to study cells in culture. Methods Cell Biol *57*, 297-311.

Quintero-Quiroz, C., Acevedo, N., Zapata-Giraldo, J., Botero, L.E., Quintero, J., Zárate-Triviño, D., Saldarriaga, J., and Pérez, V.Z. (2019). Optimization of silver nanoparticle synthesis by chemical reduction and evaluation of its antimicrobial and toxic activity. Biomaterials Research *23*, 27.

Saura, J., Tusell, J.M., and Serratosa, J. (2003). High-yield isolation of murine microglia by mild trypsinization. Glia *44*, 183-189.

Schlachet, I., and Sosnik, A. (2019). Mixed Mucoadhesive Amphiphilic Polymeric Nanoparticles Cross a Model of Nasal Septum Epithelium in Vitro. ACS Applied Materials & Interfaces *11*, 21360-21371.

Seibenhener, M.L., and Wooten, M.W. (2012). Isolation and culture of hippocampal neurons from prenatal mice. J Vis Exp *65*, 3634.

Zaritski, A., Castillo-Ecija, H., Kumarasamy, M., Peled, E., Sverdlov Arzi, R., Carcaboso, Á.M., and Sosnik, A. (2019). Selective Accumulation of Galactomannan Amphiphilic Nanomaterials in Pediatric Solid Tumor Xenografts Correlates with GLUT1 Gene Expression. ACS Applied Materials & Interfaces *11*, 38483-38496.